Disorder-induced unbinding in confined geometries

Joachim Krug[1] and Lei-Han Tang[2]
[1]*Institut für Festkörperforschung, Forschungszentrum Jülich, D-52425 Jülich, Germany*
[2]*Institut für Theoretische Physik, Universität zu Köln, Zülpicher Strasse 77, D-50937 Köln, Germany*
(Received 2 March 1994)

We consider the disorder-induced fluctuations of a directed polymer confined between two walls with attractive contact potentials. For two-dimensional systems we exploit the mapping to a one-dimensional driven lattice gas with open boundaries to obtain exactly the phase diagram as well as critical exponents and scaling functions characterizing the unbinding transitions. The competition between two attractive walls gives rise to coexistence fluctuations in the bound phase, corresponding to the shock fluctuations in the lattice gas. Scaling arguments are used to generalize these results to higher dimensions and different confinement geometries.

PACS number(s): 05.40.+j, 05.70.Ln, 68.45.−v, 74.60.Ge

I. INTRODUCTION

The interactions of flexible manifolds with extended defects such as walls or lines give rise to a rich variety of unbinding transitions [1]. These transitions underlie physical phenomena as diverse as wetting (the unbinding of an interface from a wall) and the depinning of a flux line from a screw dislocation in a type II superconductor [2]. They are governed by the competition between an attractive, localizing defect potential, and thermal fluctuations or bulk disorder which encourage the wandering of the manifold away from the defect.

In the present paper we study a directed polymer—an oriented, flexible line—subject to uncorrelated bulk disorder, and confined between *two* walls which exert attractive short range forces. The directed polymer in a random medium (DPRM) has generated much interest as a toy problem of disordered systems [3–5]. More recently, it has been studied extensively as a simple model for single flux lines in disordered superconductors; in that context the competition between extended defects and bulk disorder is of great importance [2,6].

Perhaps the most intriguing feature of the DPRM is its equivalence to stochastic growth models and (in one transverse dimension) driven lattice gases [5]. This mapping between a nonequilibrium, time-dependent process and an equilibrium system with frozen disorder is conceptually very simple: Starting from a d-dimensional nonequilibrium system, the time axis is included in the description as the $(d+1)$th coordinate; the noise histories that govern the stochastic time evolution are thus transformed into a random potential in $(d+1)$-dimensional space, and the time evolution itself is encoded (in a way to be specified below) by optimal paths (or polymers) directed along the time axis. The mapping can be formulated both in the continuum [7–9] and, via the probabilistic concept of first passage percolation [5,10,11], on the level of discrete lattice models.

Recasting the $(1+1)$-dimensional DPRM into the lattice-gas language, it is found that the two walls confining the polymer correspond to the free ends of the one-dimensional lattice on which the stochastic dynamics evolves, and the contact potentials govern the rates at which lattice-gas particles are injected at one end of the system, and removed at the other [12]; the lattice gas is totally asymmetric, i.e., particles hop in one direction only. In a remarkable series of papers, Derrida, Domany and co-workers [13–15] recently presented a complete, exact solution for this class of models. Here, our primary goal is to interpret the lattice-gas results in terms of the disorder-induced fluctuations of a directed polymer confined between two walls. Our motivation is twofold. First, we provide a new perspective on the various boundary-induced phase transitions [12] observed in the driven lattice gas, by showing that they are, in essence, manifestations of unbinding transitions [16]. Second, by exploiting the exact lattice-gas solution we confirm and extend previous (nonrigorous) work on disorder-induced unbinding in two dimensions [1,17–19].

Surprising effects arise in the bound phase when the attractive potential has the same strength at both walls: Fluctuating back and forth across the strip, the directed polymer induces an effective attraction between the walls which decays as a power of the wall separation; in the absence of disorder the corresponding dependence is exponential [20]. Within the DPRM picture, these and other features of the lattice-gas solution can be derived from simple scaling arguments, which are easily extended to higher dimensions and different confinement geometries. In higher dimensions the mapping to driven lattice gases is lost, however our results still have interesting implications for the growth of interfaces with nontrivial boundary conditions [21].

The paper is organized as follows. We begin by recalling the mapping of the DPRM to growing interfaces and driven lattice gases. Next, in Sec. III, we show how the phase diagram and the localization length for the unbinding transition can be extracted from the lattice-gas solution. We compare the results with the behavior at *thermal* unbinding in the same geometry, which is obtained from the solution of the noiseless Burgers equation or, equivalently, the mean field theory of the driven lat-

tice gas [12,13]. In Sec. IV we focus on the behavior in the bound phase with attractive walls of comparable strength, which is related to the *shock fluctuations* of the lattice gas. We develop scaling arguments that reproduce and generalize the exact results, and emphasize that the *bulk* disorder is in fact irrelevant for these effects. Section V summarizes our findings and provides an outlook onto the unbinding transition in higher dimensions. The relevant properties of the exact solution of the lattice-gas problem are derived in the Appendix.

II. THREE EQUIVALENT PROBLEMS

In this section we review the mapping of the DPRM to growing surfaces, and, in the special case of $(1+1)$ dimensions, the connection of the two to the driven lattice gas. We are particularly interested in finding conditions on the growing surface and driven lattice gas that are equivalent to the effect of confining walls in the DPRM. For this purpose it is useful to examine first a lattice version of the directed polymer problem at zero temperature.

A. Mapping among lattice models

Consider a square lattice tilted by 45° as shown in Fig. 1. Let i and j be the horizontal and vertical coordinates of a site, respectively, measured in units of $1\sqrt{2}$ times the lattice spacing. Each lattice site (i,j) is assigned independently a random energy $\epsilon(i,j)$ drawn from a distribution $P_\epsilon(x)$. A directed polymer is represented by an upward-directed path on the lattice. The energy of the directed polymer is simply the sum of the site energies on the path [3]. Denoting by $E(i,j)$ the ground state energy of the directed polymer with its upper end fixed at site (i,j), it is easy to see that the following equality holds [3,22],

$$E(i,j)=\epsilon(i,j)+\min\{E(i-1,j-1),E(i+1,j-1)\} . \tag{2.1}$$

Suppose now the directed polymer is confined by hard walls located at $i=0$ and $i=L+1>0$. Equation (2.1) still holds for $2\le i\le L-1$, but at $i=1$ and $i=L$ it is replaced by

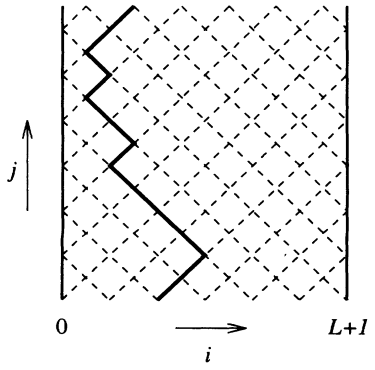

FIG. 1. Sketch of the two-dimensional lattice used in this work. The bold line indicates a directed polymer configuration.

$$E(1,j)=\epsilon(1,j)+E(2,j-1) ,$$
$$E(L,j)=\epsilon(L,j)+E(L-1,j-1) . \tag{2.2}$$

Equations (2.1) and (2.2) remain valid when the distribution $P_\epsilon(x)$ is site dependent.

Let us now turn to a surface growth problem known as the single-step model on the square lattice [23]. A surface configuration is a spanning path from left to right, specified by the column heights $j=h(i), i=1,\ldots,L$. The condition of no overhangs implies $h(i+1)-h(i)=\pm 1$. The growth process can be formulated as follows. Suppose that, at a given moment, the condition $h(i)=h(i-1)-1=h(i+1)-1$ is fulfilled. Growth $h(i)\to h(i)+2$ takes place in the next time interval dt with a probability dt. A separate description is needed for the boundary columns. Of particular interest here is that of *free boundaries*. In this case, column 1 is ready to grow if $h(1)=h(2)-1$. For reasons which will become clear later, we assign a growth probability $\alpha\,dt$ in a time interval dt to this column. Similarly, column L is ready to grow if $h(L)=h(L-1)-1$, with a growth probability $\beta\,dt$ in a time interval dt.

Denoting by $t(i,j)$ the time at which the surface reaches site (i,j), the following relation is observed to hold:

$$t(i,j)=\tau(i,j)+\max\{t(i-1,j-1),t(i+1,j-1)\} . \tag{2.3}$$

Here $\tau(i,j)$ is the time it takes for the growth $h(i)=j-2\to h(i)=j$ to occur, starting from the moment when both sites $(i-1,j-1)$ and $(i+1,j-1)$ are on the surface, as given by the second term on the right-hand side of (2.3). For the boundary columns $i=1$ and L, Eq. (2.3) is replaced by

$$t(1,j)=\tau(1,j)+t(2,j-1) ,$$
$$t(L,j)=\tau(L,j)+t(L-1,j-1) . \tag{2.4}$$

From the definition of the growth model we see that $\tau(i,j)$ is a stochastic variable independent from site to site. The distribution of $\tau(i,j)$ for $2\le i\le L-1$ is given by

$$P_\tau(x)=e^{-x} . \tag{2.5}$$

At the boundaries, $\tau(1,j)$ is distributed according to

$$P_{\tau,1}(x)=\alpha e^{-\alpha x} , \tag{2.6}$$

while $\tau(L,j)$ is distributed according to

$$P_{\tau,L}(x)=\beta e^{-\beta x} . \tag{2.7}$$

The attentive reader would realize immediately the parallels of the DPRM and the single-step model defined above. In fact, the two are formally completely equivalent if we make the following identifications:

$$\epsilon(i,j)=-\tau(i,j),\quad E(i,j)=-t(i,j) . \tag{2.8}$$

The distribution of the site energies ϵ in the bulk is easily obtained from (2.5). At the boundary column $i=1$, we write $\epsilon(1,j)=\epsilon_B(1,j)+V(j)$, where ϵ_B obeys the distribution of site energies in the bulk. Using (2.5) and (2.6) it is easy to verify that, for $\alpha<1$, the distribution of $V\le 0$ is given by

$$P_V(x)=\alpha\delta(x)+\alpha(1-\alpha)e^{\alpha x} . \quad (2.9)$$

Thus the case $\alpha<1$ corresponds to an attractive potential next to the left wall. Similarly, the case $\beta<1$ corresponds to an attractive potential next to the right wall.

The surface height $h(i,t)$ in the single-step model can (in principle) be obtained from the solution of the directed polymer problem by inverting the equation

$$E(i,h)=-t . \quad (2.10)$$

At long times (or equivalently, for long polymers), one may write, to leading order, $E(i,j)\simeq e_0 j$ and $h(i,t)\simeq vt$. Here e_0 is the ground state energy per unit length of an infinite directed polymer, and v is the steady-state growth velocity. From (2.10) we obtain

$$v=-1/e_0 . \quad (2.11)$$

Finally, we recall the lattice-gas analogy of the single-step model [5]. Let

$$\sigma_i\equiv[1+h(i)-h(i+1)]/2 \quad (2.12)$$

denote the occupation number of site i on a one-dimensional chain, $i=1,\ldots,L-1$. Due to the single-step constraint, σ_i takes only two possible values, 0 and 1. The condition for growth of column i corresponds to $\sigma_{i-1}=1$ and $\sigma_i=0$. Growth $h(i)\to h(i)+2$ changes the occupation numbers to $\sigma_{i-1}=0$ and $\sigma_i=1$, i.e., a particle jumps from site $i-1$ to site i on the chain. The probability for the jump to occur in a time interval dt is dt. At site 1, growth $h(1)\to h(1)+2$ corresponds to feeding in a particle from outside, and this is done with a probability $\alpha\,dt$ in a time interval dt. Similarly, growth $h(L)\to h(L)+2$ at column L corresponds to taking away a particle at site $L-1$ on the chain, which is done with probability $\beta\,dt$ in a time interval dt. This is precisely the model studied in Refs. [12–15]. Knowing the lattice-gas configuration, one can easily reconstruct the surface configuration using

$$h(i)=h(1)+\sum_{k=1}^{i-1}(1-2\sigma_k) . \quad (2.13)$$

Since for every lattice-gas jump the surface advances by two lattice units, the lattice-gas current is related to the growth velocity by $J=v/2$, and to the DPRM ground state energy through

$$J=-(2e_0)^{-1} . \quad (2.14)$$

The mapping between the DPRM at zero temperature and a certain class of surface growth problems carries through to higher dimensions (see Ref. [25]). As the gradient of the height is no longer a scalar in higher dimensions, these surface growth models do not coincide with direct generalizations of the one-dimensional driven lattice gas [5].

B. Continuum formulation

Although the models on lattice discussed above have the virtue of being easily implementable on a computer and, in the case of the lattice-gas problem, able to afford an exact solution, additional physical insights can be gained from the continuum formulation of these problems. In this language, the configuration of the directed polymer is specified by its transverse displacements $\mathbf{x}(t)$, where t is the coordinate along the preferred direction. The energy of the directed polymer is given by

$$H=\int_{t_1}^{t_2}dt\left[\frac{\gamma}{2}\left|\frac{d\mathbf{x}}{dt}\right|^2+\eta(\mathbf{x},t)+V(\mathbf{x})\right] . \quad (2.15)$$

Here γ is the line tension, $\eta(\mathbf{x},t)$ is a Gaussian random potential with zero average and covariance

$$\langle\eta(\mathbf{x},t)\eta(\mathbf{x}',t')\rangle=2D\delta^d(\mathbf{x}-\mathbf{x}')\delta(t-t') , \quad (2.16)$$

and $V(\mathbf{x})$ is a t-independent potential.

The partition function of the directed polymer with its upper end fixed at $(\mathbf{x},t)$ is given by

$$Z(\mathbf{x},t)=\sum_P\exp(-H_P/k_BT) , \quad (2.17)$$

where the sum is over all possible configurations P of the directed polymer ending at $(\mathbf{x},t)$. Using (2.15), it is easy to verify that Z satisfies the Schrödinger equation in imaginary time,

$$-\frac{\partial Z}{\partial t}=\frac{1}{k_BT}\left[-\frac{(k_BT)^2}{2\gamma}\nabla^2+\eta(\mathbf{x}t)+V(\mathbf{x})\right]Z . \quad (2.18)$$

Under the Hopf-Cole transformation $Z=\exp(-F/k_BT)$, one arrives at the Kardar-Parisi-Zhang (KPZ) equation for the free energy $F(\mathbf{x},t)$ [7,8],

$$\frac{\partial F}{\partial t}=\frac{k_BT}{2\gamma}\nabla^2F-\frac{1}{2\gamma}(\nabla F)^2+V(\mathbf{x})+\eta(\mathbf{x},t) . \quad (2.19)$$

In the context of surface growth, F has the interpretation of surface height. An attractive potential ($V<0$) corresponds to a reduced growth rate, while a repulsive potential ($V>0$) corresponds to an enhanced growth rate [24]. In the $(1+1)$-dimensional case, the equation satisfied by ∇F is known as the noisy Burgers equation whose connection to the driven lattice-gas problem has been well documented [26].

III. UNBINDING TRANSITIONS

A. Phase diagram

The thermodynamic properties of the system are determined by the ground state energy per unit length, e_0, which is related to the lattice-gas current through (2.14). We discuss here the dependence of this quantity on the boundary parameters α and β, keeping in mind that the average boundary energies are $\langle\epsilon(1,j)\rangle=-1/\alpha$, $\langle\epsilon(L,j)\rangle=-1/\beta$, while the bulk energy is fixed at $\langle\epsilon(i,j)\rangle=-1$.

It is shown in the Appendix that the ground state energy can be written as the ratio of two matrix elements [Eq. (A2)], each of which has three contributions I_1, I_2 and I_3 [Eq. (A6)]. For $\alpha,\beta>1/2$, $I_1\sim 4^L$ is the only contribution [cf. (A15)], while for $\alpha<\frac{1}{2},\alpha<\beta$ the dominant term is $I_2\sim[\alpha(1-\alpha)]^{-L}$ [Eq. (A10)] and for $\beta<\frac{1}{2},\beta<\alpha$ the

term $I_3 \sim [\beta(1-\beta)]^{-L}$ dominates [Eq. (A11)]. Using only these leading behaviors we obtain [14,15]

$$e_0 = \begin{cases} -2, & \alpha,\beta \geq \frac{1}{2} \\ -[2\alpha(1-\alpha)]^{-1}, & \alpha < \frac{1}{2}, \alpha < \beta \\ -[2\beta(1-\beta)]^{-1}, & \beta < \frac{1}{2}, \beta < \alpha \end{cases} \quad (3.1)$$

a result which also follows from mean field approximations [12,13] and simple physical considerations [12,15] applied to the lattice gas.

The phase diagram is depicted in Fig. 2. In the upper right part $\alpha,\beta > \frac{1}{2}$ the polymer is unbound, and consequently e_0 is independent of the boundary energies. At $\alpha = \frac{1}{2}$ ($\beta = \frac{1}{2}$) the polymer undergoes an unbinding transition at the left (right) wall. When $\alpha < \frac{1}{2}$ *and* $\beta < \frac{1}{2}$ the polymer is bound at the more attractive wall, and the ground state energy depends only on the contact potential of that wall. The unbinding transitions are of second order, in the sense of continuous first derivatives $\partial e_0/\partial(\alpha,\beta)$, and the singular part of the ground state energy vanishes quadratically as the transition is approached from the bound side, in agreement with Kardar's replica calculation [17]. The singularity is the *same* as the free energy singularity in thermal unbinding [1,17]. In the lattice-gas context this corresponds precisely to the fact that the ground state energy (3.1) is given *exactly* by the mean field approximation (cf. Sec. III C).

The additional feature due to the presence of two walls is the transition along the line $\alpha = \beta < \frac{1}{2}$, which is a *coexistence line* connecting the two bound phases. Despite being of first order [in the sense of a discontinuous first derivative of $e_0(\alpha,\beta)$], this transition is associated with a diverging correlation length, as will be demonstrated in the following section. The underlying physics is explained in Sec. IV.

B. Confinement energies and localization lengths

In order to more fully characterize the unbinding transitions and extract the appropriate diverging length scales

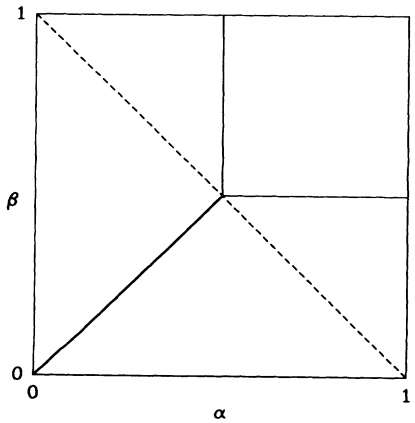

FIG. 2. Phase diagram. Full lines are second order unbinding transitions. Along the bold line two bound phases coexist. At the dashed line $\alpha+\beta=1$ the confinement energy changes its sign.

we need to go beyond the thermodynamic description and consider fluctuation quantities. We have found that the most convenient quantity for this purpose is the *confinement energy*, i.e., the shift $\Delta e(L)$ in the ground state energy e_0 due to the lateral confinement of the polymer to a strip of width L. The length of the polymer remains infinite; this is necessary because the exact solution of the lattice-gas model [13–15] covers only the stationary ($t \to \infty$) regime.

Quite generally, the lateral confinement of a flexible line on a scale L requires an energy cost $\Delta e(L) \sim L^{-\tau}$ with $\tau = 2(1-\zeta)/\zeta$ in terms of the wandering exponent ζ of the line [27]. The exact (1+1)-dimensional DPRM wandering exponent $\zeta = \frac{2}{3}$ [5,8] thus implies $\tau = 1$, and we expect, to leading order in $1/L$,

$$\Delta e(L) = e_0(L) - e_0(\infty) \approx \frac{2c}{L} . \quad (3.2)$$

The coefficient c in (3.2) is universal, in the following sense: Simple considerations [21] applied to the continuum Eq. (2.19) in (1+1) dimensions show that the leading finite size correction to the free energy per unit length $f_0 = \lim_{t\to\infty} \langle \partial F/\partial t \rangle$ is of the form

$$\Delta f = c \frac{D}{k_B T} \frac{1}{L} , \quad (3.3)$$

where the ratio $D/k_B T$ is a model-dependent quantity that can be determined from certain correlation functions [28]; for the present model $D/k_B T = -e_0(\infty) = 2$. In contrast, the amplitude c should depend only on the type of lateral boundary conditions. For periodic boundary conditions (confinement on a cylinder) it has been shown that $c = 1$ [21].

In the unbound phase, $\Delta e(L)$ can be determined by expanding (A15) for large u,v, using the asymptotics (A21) of the scaling function F. The result is $e_0 = -2[1 - \frac{3}{2}L^{-1} + O(L^{-2})]$, which is precisely of the form (3.2) with $c = \frac{3}{2}$. Moreover, this value is seen to apply to the whole unbound phase $\alpha,\beta > \frac{1}{2}$ [29]. At the unbinding transitions ($\alpha = \frac{1}{2} < \beta$ or $\beta = \frac{1}{2} < \alpha$) one has to set $u = 0$ or $v = 0$ in (A15), which leads to $e_0 = -2[1 - \frac{1}{2}L^{-1} + O(L^{-2})]$; hence $c = \frac{1}{2}$ if one of the two walls is at the critical point.

In the bound phase the confinement due to the second wall should be less important, and we expect the confinement energy to vanish rapidly with increasing L. More precisely, it should behave as $\Delta e \sim \exp(-L/\xi)$, where ξ is the localization length of the polymer. To compute the finite size correction for $\alpha < \frac{1}{2} < \beta$ (the case $\beta < \frac{1}{2} < \alpha$ is of course completely analogous), we need to include both the leading (I_2) and subleading (I_1) contributions to the matrix elements in the evaluation of (A2). For large L, the result can be written as

$$\Delta e \simeq \frac{1}{2\sqrt{\pi}} \frac{(\beta-\alpha)(\alpha+\beta-1)}{\alpha(1-\alpha)(1-2\alpha)(1-2\beta)^2} \frac{e^{-L/\xi_\alpha}}{L^{3/2}} , \quad (3.4)$$

where we have introduced the localization length

$$\xi_\alpha = (-\ln[4\alpha(1-\alpha)])^{-1} . \quad (3.5)$$

Upon approaching the transition, $\alpha \to \frac{1}{2}$, but keeping $L \gg \xi_\alpha$, (3.4) reduces to

$$\Delta e \simeq \frac{1}{2\sqrt{\pi}} \frac{1}{L} \left[\frac{\xi_\alpha}{L} \right]^{1/2} e^{-L/\xi_\alpha} \tag{3.6}$$

and the localization length diverges quadratically, $\xi_\alpha \sim (\alpha_c - \alpha)^{-\psi}$ with $\psi = 2$ and $\alpha_c = \frac{1}{2}$. This provides the first *rigorous* confirmation of the value $\psi = 2$ of the unbinding exponent predicted by the replica analysis [17] as well as by the necklace model [27], which suggests that $\psi = \zeta/(1-\zeta)$ in general. For $\xi_\alpha \sim L$ (3.6) crosses over to the $1/L$-behavior characteristic of the unbound phase.

It is interesting to note that the diverging localization length plays a role also when the unbinding transition is approached from the unbound side. As was pointed out above, $e_0 \simeq -2(1-\frac{3}{2}L^{-1})$ in the unbound phase, while $e_0 \simeq -2(1-\frac{1}{2}L^{-1})$ at the transition. The crossover is described by, for $\xi_\alpha \gg 1$ and $\xi_\beta = -\ln^{-1}[4\beta(1-\beta)] \ll \xi_\alpha, L$,

$$e_0 \simeq -2 \left[1 - \frac{1}{2L} \left[1 + \frac{\pi^{1/2}\sqrt{L/\xi_\alpha} F'(\sqrt{L/\xi_\alpha})}{1 - \pi^{1/2} F(\sqrt{L/\xi_\alpha})} \right] \right], \tag{3.7}$$

with the scaling function F defined in (A18).

We are now prepared to explain the significance of the dashed line $\alpha+\beta=1$ in the phase diagram (Fig. 2). Along that line, the steady state of the lattice gas becomes trivial in the sense that it is *indistinguishable* from the state of a finite piece of an infinite system [14,15]. In particular, the confinement energy Δe vanishes identically for any strip width L, as can also be seen from the asymptotic expression (3.4). Our interpretation of this phenomenon is as follows: When $\alpha+\beta=1$, the potential of the confining wall matches that of the localizing wall such that the probability for the polymer to be located at the confining wall takes precisely the value it would take in a semi-infinite geometry. As we shall see in Sec. III C, the same effect appears in thermal unbinding.

For $\alpha+\beta<1$ the confinement energy is negative [cf. Eq. (3.4)]. Consequently, the effective force $-\partial e_0/\partial L$ exerted by the fluctuating polymer on the confining walls becomes *attractive*. In particular, this is true in the regime $\alpha,\beta<\frac{1}{2}$, where the dominant contributions to the matrix element (A6) are I_2 and I_3. Using the exact expressions (A10) and (A11) we obtain, for large L and $\alpha<\beta$,

$$\Delta e = -\frac{(1-2\beta)(\beta-\alpha)(1-\beta-\alpha)}{2(1-2\alpha)\alpha(1-\alpha)\beta(1-\beta)} e^{-L/\tilde{\xi}} + O(e^{-L/\xi_\alpha}), \tag{3.8}$$

where we have introduced a new length scale $\tilde{\xi}$ defined by

$$\tilde{\xi}^{-1} = \ln \left[\frac{\beta(1-\beta)}{\alpha(1-\alpha)} \right]. \tag{3.9}$$

As pointed out by Schütz and Domany [15], $\tilde{\xi}^{-1} = \xi_\alpha^{-1} - \xi_\beta^{-1}$, where $\xi_{\alpha,\beta}$ are the localization lengths associated with the two bound phases which meet at the coexistence line, defined through (3.5). This makes it possible for $\tilde{\xi}$ to *diverge* close to coexistence, despite the fact that the localization lengths in both phases remain finite. Indeed, in the limit $\alpha \to \beta - 0$ we have

$$\tilde{\xi} \approx \frac{\alpha(1-\alpha)}{(1-2\alpha)} (\beta-\alpha)^{-1} \tag{3.10}$$

and (3.8) reduces to, for $\tilde{\xi} \ll L$,

$$\Delta e \simeq -\frac{1}{2\alpha(1-\alpha)} \tilde{\xi}^{-1} e^{-L/\tilde{\xi}}. \tag{3.11}$$

At coexistence, $\alpha = \beta < \frac{1}{2}$, the ground state energy is given exactly by (up to exponentially small corrections of order e^{-L/ξ_α})

$$e_0 = -\frac{1}{2\alpha(1-\alpha)} \left[\frac{2\alpha(1-\alpha) + L(1-2\alpha)^2}{2\alpha(1-\alpha) + (L-1)(1-2\alpha)^2} \right]. \tag{3.12}$$

Far away from the critical point $\alpha = \frac{1}{2}$, i.e., for $\xi_\alpha \ll L$, this reduces to a confinement energy

$$\Delta e = -\frac{1}{2\alpha(1-\alpha)} \frac{1}{L}, \tag{3.13}$$

which (up to the sign) is reminiscent of the $1/L$ behavior in the unbound phase. However, we will show in Sec. IV that the origin of the confinement energy is quite different in the two cases. In particular, in higher dimensions the two quantities are expected to scale with different powers of L. Approaching the critical point $\alpha = \beta = \frac{1}{2}$ along the coexistence line deviations from (3.13) show up when $\xi_\alpha \approx (1-2\alpha)^{-2} \sim L$.

C. Thermal unbinding and mean field theory

The results of the previous section can be put into perspective by comparing them to the *thermal* unbinding of a directed polymer (or a one-dimensional interface) confined between two walls. This problem is most conveniently treated in the continuum formulation of Sec. II B. In the thermal case the random potential $\eta(x,t)$ in (2.19) is omitted. Moreover, for simplicity we replace the effect of the wall potential $V(x)$ by the boundary conditions [1]

$$Z'(0,t)/Z(0,t) = -l_0^{-1}, \quad Z'(L,t)/Z(L,t) = l_L^{-1} \tag{3.14}$$

for the restricted partition function, where $l_0 > 0$ ($l_L > 0$) when the polymer is bound at $x = 0$ ($x = L$) and $l_0 < 0$ ($l_L < 0$) is the unbound case. In the bound regime this mimics the exponential decay of the partition function outside of the interaction range of the wall potential. Elementary quantum mechanics [1] shows that $l_{0,L} \sim |V_{0,L} - V_c|^{-1}$ as the potential strength approaches its critical value from above. Close to the transition the boundary parameters in (3.14) are therefore related to those of the disordered lattice problem through $l_0^{-1} \sim \frac{1}{2} - \alpha$, $l_L^{-1} \sim \frac{1}{2} - \beta$ [see (3.17)].

In the stationary regime, $t \to \infty$, the free energy per unit length $f_0 = \partial F/\partial t$ is determined by the stationary

solution of (2.19) with $\eta=V=0$ and the appropriate boundary conditions. The problem further simplifies by introducing the function $u=\partial F/\partial x$. This quantity is independent of time and satisfies

$$k_BT\frac{du}{dx}=u^2+2\gamma f_0 \tag{3.15}$$

with the boundary conditions $u(0)=u_0=k_BT/l_0$ and $u(L)=u_L=-k_BT/l_L$. Hence f_0 is given implicitly as a function of L, l_0, and l_L through the relation

$$L=k_BT\int_{u_0}^{u_L}\frac{du}{u^2+2\gamma f_0}\ . \tag{3.16}$$

The behavior in the thermodynamic limit is obtained by tuning f_0 such that the integrand on the right-hand side of (3.16) diverges, either at $u=0$ or at one of the boundaries. The resulting phase diagram is *identical* to that of the disordered system (Fig. 2) if we set

$$\alpha=\tfrac{1}{2}-u_0,\quad \beta=\tfrac{1}{2}+u_L\ . \tag{3.17}$$

The unbound phase occupies the region $u_L>0>u_0$, where $f_0=0$ in the thermodynamic limit. The unbinding transition at $x=0$ ($x=L$) occurs along the line $u_0=0, u_L>0$ ($u_L=0, u_0<0$). The free energy is equal to $f_0=-u_0^2/2\gamma=-(k_BT/l_0)^2/2\gamma$ when the polymer is bound at $x=0$ (in the region $u_0>0, u_L>-u_0$), and equal to $f_0=-(k_BT/l_L)^2/2\gamma$ for $u_L<0, u_L<-u_0$. As before, the free energy vanishes *quadratically* (in $l_{0,L}^{-1}$ and hence in $|V_{0,L}-V_c|$) at the transition. The coexistence line is located at $u_0=-u_L>0$. Finally, the significance of the dotted line $u_0=u_L$ is obvious from (3.16): Along that locus, the solution of (3.15) becomes trivial, $f_0=-u_0^2/2\gamma$ with *no* finite size corrections.

The finite size corrections to the free energy are easily computed from (3.16). In the unbound phase we find a power-law confinement energy

$$\Delta f=f_0(L)-f_0(\infty)=\frac{1}{2\gamma}\left[\frac{c\pi k_BT}{L}\right]^2, \tag{3.18}$$

where $c=1$ for $u_0<0<u_L$ and $c=\frac{1}{2}$ when one of the two walls is at its unbinding transition. Note that in the latter case the confinement energy is simply that of a completely unbound polymer in a strip of width $2L$, as could have been guessed from the boundary conditions (3.14); the corresponding result for the disordered system (Sec. III B) does not have such a straightforward interpretation. The $1/L^2$ decay of Δf conforms to the scaling prediction $\tau=2(1-\zeta)/\zeta=2$ for thermal roughening [27].

When the polymer is bound at $x=0, u_0>0$, the confinement free energy is exponentially small in L/l_0 and given by

$$\Delta f=-2\frac{(k_BT)^2}{\gamma l_0^2}\frac{l_L+l_0}{l_L-l_0}e^{-2L/l_0}\ . \tag{3.19}$$

In terms of (3.17) the dimensionless prefactor in (3.19) is equal to $(1-\beta-\alpha)/(\beta-\alpha)$. Two features are noteworthy. First, Δf changes sign at the dotted line in Fig. 2 ($l_L=-l_0$ in present units), signaling the transition from repulsive to attractive confinement effects. Second, the prefactor of (3.19) diverges upon approaching the coexistence line where $l_L=l_0>0$. At coexistence, $u_0=-u_L>0$, the evaluation of (3.16) yields

$$\Delta f=-2\frac{(k_BT)^2}{\gamma l_0^2}e^{-L/l_0}\ . \tag{3.20}$$

Comparison with the exponential factor of (3.19) shows that the effective system size at coexistence is $L/2$ or, equivalently, the effective localization length is doubled. Moreover, we see that the crossover from (3.19) to (3.20) occurs when $L\sim\tilde{\xi}$ with

$$\tilde{\xi}=l_0\ln\left[\frac{2l_L}{l_L-l_0}\right]\ . \tag{3.21}$$

Thus, a diverging length scale can be associated with the coexistence line both in thermal and disorder-induced unbinding, however here the power-law divergence of $\tilde{\xi}$ derived in Sec. III B [Eq. (3.10)] is replaced by logarithmic behavior. As will be shown in Sec. IV B, the difference can be traced back to the fact that the coexistence fluctuations in the thermal case are of entropic origin.

Finally, we show that the present treatment of thermal unbinding is completely equivalent to the mean field theory of the driven lattice gas [12,13,30,31]. In its continuum formulation [12,30,31] the mean field theory starts from an expression for the total current as a function of the local density $\rho(x)=\langle\sigma_x\rangle$ [cf. (2.12)],

$$J=\rho(1-\rho)-D_{\mathrm{MF}}\frac{\partial}{\partial x}\rho\ . \tag{3.22}$$

Here the first, systematic term is known to become exact in the infinite bulk system, while the second term represents a phenomenological diffusive contribution [12,30]. The boundary rates α and β essentially fix the boundary densities through $\rho(0)=\alpha$, $\rho(L)=1-\beta$. Together with these boundary conditions the stationarity condition (3.22) determines the current as well as the density profile. With the idenfications $\frac{1}{2}-\rho\to u$, $D_{\mathrm{MF}}\to k_BT$, and $J-\frac{1}{4}\to 2\gamma f_0$, this problem reduces to the one solved above.

We note in passing that the correct scaling properties of the disordered system can be obtained from a modified mean field theory in which the diffusion constant D_{MF} becomes scale dependent [12]. The one feature which *cannot* be reproduced by this heuristic method is the behavior close to the coexistence line $\alpha=\beta$. This is the topic of the following section.

IV. COEXISTENCE FLUCTUATIONS

The comparison with the thermal case in the preceding section indicates that the behavior of the disordered model close to the coexistence line $\alpha=\beta$ depends essentially on the presence of randomness. More precisely, we will argue that the crucial ingredient are the disorder fluctuations close to the localizing wall.

A. Shock fluctuations

In the lattice-gas context the behavior on the coexistence line $\alpha=\beta$ is characterized by *shock fluctuations:* Typical configurations consist of regions of low density $\sigma_i \approx \alpha < \frac{1}{2}$ for $0<i<x_0$, separated by a microscopically sharp shock from the high density region $x_0<i<L$, where $\sigma_i \approx 1-\alpha > \frac{1}{2}$ [14,15,32]. The shock position x_0 is found with equal probability anywhere in the system. Consequently, the *averaged* density profile increases linearly from $\langle \sigma_1 \rangle = \alpha$ to $\langle \sigma_L \rangle = 1-\alpha$, however the average is not representative of *typical* configurations [14].

From (2.13) we recognize that the corresponding typical height profiles are roof shaped, with a maximum at the shock position x_0. The behavior of the directed polymer follows from the observation that, according to (2.10), the height configurations $j=h(i,t)$ are *lines of constant ground state energy* $E(i,j)=-t$. Plotting subsequent height configurations we therefore map out the ground state energy landscape (Fig. 3). The shock position x_0 traces out the watershed which divides the domain of attraction of the left wall $i=1$ from that of the right wall $i=L$. Roughly speaking, the global energy minimum for fixed j— i.e., the position of the end point of the globally optimal path of length j—resides near the right wall when $x_0 < L/2$, and near the left wall when $x_0 > L/2$. As the shock position wanders, the energy minimum occasionally switches from one wall to the other; since the shock position performs a random walk with a diffusion constant of order unity, the switching time scale is of the order L^2 (Fig. 4).

The physical origin of the lattice-gas shock fluctuations is the imbalance between the number of particles injected at $i=1$, and the number removed at $i=L$. In the language of the directed polymer the phenomenon arises from the relative energy fluctuations between the two bound phases: While their average energies are degenerate, fluctuations are caused by the (essentially one-dimensional) disorder along each of the two localizing grooves in the energy landscape. This observation is sufficient to understand most of the scaling laws found in Sec. III B.

B. Scaling arguments

Consider first the behavior slightly off coexistence, with $\beta > \alpha$, so that the ground state configuration is localized near $i=1$. We estimate the energy of a kinklike excitation, in which a segment of length $L_\parallel$ is moved across the strip and attached to the right wall at $i=L$ (Fig. 5). The energy *cost* consists of a term of order $(e_\beta - e_\alpha)L_\parallel$ and two crossing contributions of order L, where e_α (e_β) is the energy per unit length associated with the bound phase at the left (right) wall. From (3.1) we have

$$e_\beta - e_\alpha \approx \frac{(\beta-\alpha)(1-2\alpha)}{2\alpha^2(1-\alpha)^2} \tag{4.1}$$

for $\alpha \to \beta - 0$. The polymer incurs an energy *gain* if the fluctuating part of the effective wall potentials favors the right wall over the left in the region occupied by the kink. Due to the one dimensionality of the wall, the gain is of order $L_\parallel^{1/2}$. Thus, the kink energy can be written as

$$E_{\text{kink}} = (e_\beta - e_\alpha)L_\parallel + 2e_1 L - e_2 L_\parallel^{1/2} , \tag{4.2}$$

where, away from the unbinding transition, e_1 and e_2 are positive coefficients of order unity. Minimizing with

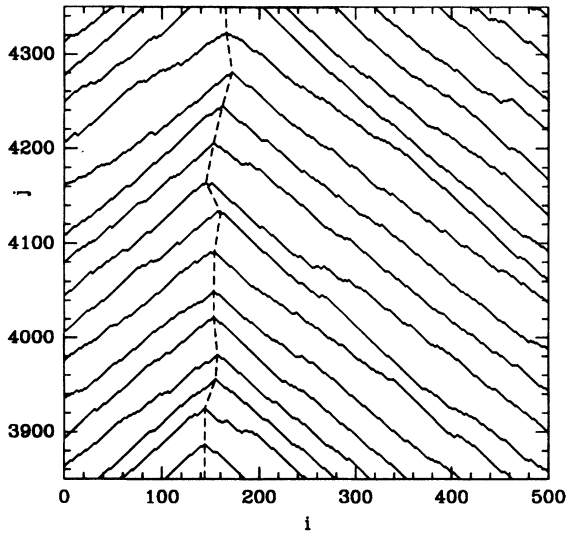

FIG. 3. The figure shows 20 subsequent snapshots of a single-step interface of length $L=500$, taken at time intervals $\Delta t = 200$. The boundary parameters were $\alpha=\beta=0.1$. These interface configurations can be viewed as level sets in the ground state energy landscape of the DPRM. The energy decreases from $E=-t=-20000$ along the bottom configuration to $E=-24000$ at the top. The dashed line maps out the watershed between the domains of attraction of the left and the right wall; in this section of the lattice the polymer remains localized at the right wall.

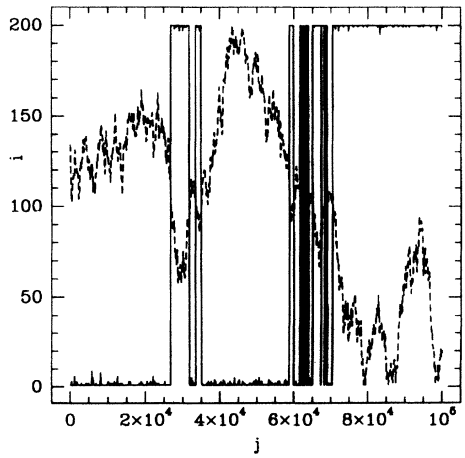

FIG. 4. Shock fluctuations. The figure shows the time evolution of the position of the maximum (dashed line) and the minimum (full line) of roof-shaped interface configurations of the kind shown in Fig. 3, however for $L=200$. The two curves approximately follow the lattice-gas shock position and the position of the global ground state of the DPRM, respectively.

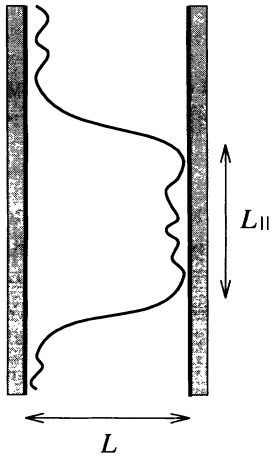

FIG. 5. Sketch of a kink excitation of a polymer bound at the (slightly more attractive) left wall.

respect to $L_{\|}$ we obtain the optimal kink size

$$L_{\|}=\frac{e_2^2\alpha^4(1-\alpha)^4}{(\beta-\alpha)^2(1-2\alpha)^2} . \tag{4.3}$$

Clearly a kink will form only if $E_{\rm kink}$, evaluated at the optimal kink size, is negative. This occurs when $L<L_{\perp}$, where

$$L_{\perp}=\frac{(e_2^2/e_1)\alpha^2(1-\alpha)^2}{4(\beta-\alpha)(1-2\alpha)} \tag{4.4}$$

can be identified with the correlation length $\tilde{\xi}$ introduced in Sec. III B. We have thus recovered the divergence $\tilde{\xi}\sim|\beta-\alpha|^{-1}$ derived in (3.10).

Next we determine the confinement energy at coexistence. We expect the optimal configuration of a polymer of length j to consist of N kinks and antikinks of length $L_{\|}$ with $NL_{\|}=j$. Each kink incurs an energy gain of order $L_{\|}^{1/2}$, and an energy cost of order L. The total energy change per unit length, as compared to a configuration localized near a single wall, is then

$$\Delta e=e_1L/L_{\|}-e_2L_{\|}^{-1/2} . \tag{4.5}$$

The optimal kink size is now

$$L_{\|}=4(e_1/e_2)^2L^2 \tag{4.6}$$

and inserting into (4.5) we obtain an attractive confinement energy of order $1/L$,

$$\Delta e=-\frac{1}{4}\left[\frac{e_2^2}{e_1}\frac{1}{L}\right] , \tag{4.7}$$

in agreement with (3.13).

It should have become clear that these arguments do not involve the disorder in the bulk of the system. Bulk properties enter only through the coefficient e_1 in (4.2), (4.5), which expresses the fact that the *average* energy of the bulk exceeds that of the boundaries. Consequently, the coexistence fluctuation effects should persist even in the absence of bulk disorder, as long as the wall potentials have a random component. This expectation is corroborated by the work of Schütz [33], who studied a lattice-gas model where particles are randomly injected and removed at rates α and β, respectively, but move deterministically in the bulk. Along the lines of Sec. II A this maps onto a zero temperature directed polymer problem with random site energies along the boundary rows $i=1$ and $i=L$, and fixed (nonrandom) energies in the bulk. Clearly in the absence of bulk disorder (and thermal fluctuations) there are no unbinding transitions and the whole parameter space $0\le\alpha,\beta\le1$ is occupied by the two localized phases, analogous to the lower left corner of Fig. 2. Nevertheless, close to the coexistence line $\alpha=\beta$ the results of Schütz reduce *exactly* to the asymptotic expressions (3.11) and (3.13), if the bulk energy $e_0=\min(-1/2\alpha,-1/2\beta)$ and the correlation length $\tilde{\xi}=\ln^{-1}(\beta/\alpha)\approx\alpha/(\beta-\alpha)$ appropriate for Schütz's model are inserted. Thus these results appear to posses a certain degree of universality.

We now turn to the behavior of the coexistence fluctuations as the unbinding transition is approached along the coexistence line $\alpha=\beta<\frac{1}{2}$ (Fig. 2). The coefficients e_1 and e_2 in (4.5) are expected to become singular at $\alpha=\alpha_c=\frac{1}{2}$. Consider first the crossing energy e_1. Two competing effects have to be taken into account. As $\alpha\to\alpha_c$, the energy difference between the bound phases and the unbound phase vanishes as $(\alpha_c-\alpha)^2$ (Sec. III A), however, at the same time the segments of the polymer that cross the strip tend to align with the walls. To see this, let ϕ denote the angle enclosed by these crossing segments and the wall. Then the length of a segment is $L_s=L/\phi$ for small ϕ, and hence $e_1\approx(\alpha_c-\alpha)^2/\phi$. To determine ϕ, we note that the tilting of the crossing segment relative to the average direction of the polymer incurs an elastic energy cost of the order $L^2/L_s=L\phi$ per unit length [4]. Including this term into (4.5) and minimizing with respect to ϕ we find that ϕ vanishes as $\phi\sim\alpha_c-\alpha$. Therefore,

$$e_1\sim\alpha_c-\alpha . \tag{4.8}$$

Next consider the effect of the unbinding transition on the fluctuations in the bound phase, described by the coefficient e_2. We first recall that, in addition to the localization length $\xi\sim(\alpha_c-\alpha)^{-2}$ (cf. Sec. III B), a diverging correlation length *parallel* to the walls,

$$\xi_{\|}\sim\xi^{1/\zeta}=\xi^{3/2}\sim(\alpha_c-\alpha)^{-3} \tag{4.9}$$

can be associated with the unbinding transition [1]. Polymer segments of length $l<\xi_{\|}$ behave as in the unbound phase. In particular, the ground state energy fluctuations scale as l^{θ_1} for $l<\xi_{\|}$, where $\theta_1=\frac{1}{3}$ is the energy fluctuation exponent of the *free* DPRM [3,5,7,8]; the simple $l^{1/2}$ behavior of the fluctuations is recovered only on scales $l>\xi_{\|}$. Matching the two power laws it follows that the prefactor of the fluctuation term in (4.5) vanishes as

$$e_2\sim\xi_{\|}^{-1/6}\sim(\alpha_c-\alpha)^{1/2} . \tag{4.10}$$

Surprisingly, the combination e_2^2/e_1 that enters (4.4) and (4.7) remains constant as $\alpha\to\alpha_c$. This is nicely consistent with the exact results (3.13) and (3.10), which show that

the coefficient of the $1/L$ confinement energy remains finite upon approaching the transition, while the prefactor of the coexistence correlation length $\tilde{\xi}\sim|\alpha-\beta|^{-1}$ diverges as $(\alpha_c-\alpha)^{-1}$ [compare (3.10) with (4.4)].

Finally, it is instructive to apply similar arguments to a *thermally* excited directed polymer (or interface) confined between two equally attractive walls. Here the incentive for the configuration to switch from one wall to the other is of entropic origin. Consider a polymer of length t, which forms N kinks of length $L_\parallel$, with $t=NL_\parallel$. The positional entropy of the array of kinks is

$$S=k_B\ln(t^N/N!)\approx k_B\frac{t}{L_\parallel}(\ln L_\parallel+1)\ . \tag{4.11}$$

Together with the energy cost γL per kink the total free energy is

$$F=E-TS=t\left[\frac{\gamma L}{L_\parallel}-k_BT\frac{\ln L_\parallel+1}{L_\parallel}\right]\ . \tag{4.12}$$

Minimizing with respect to $L_\parallel$ yields an exponentially diverging correlation length

$$L_\parallel\approx e^{\gamma L/k_BT}\ , \tag{4.13}$$

which agrees (up to prefactors that the present approach to too crude to capture) with detailed calculations [20] as well as general properties of zero temperature phase transitions in one dimension. Inserting this into (4.12) one finds an attractive confinement free energy per unit length,

$$\Delta f\approx -k_BTe^{-\gamma L/k_BT} \tag{4.14}$$

as derived in (3.20). Related considerations can be used to obtain the logarithmically diverging length scale $\tilde{\xi}$ [Eq. (3.21)] characterizing the *approach* to criticality, along with a parallel correlation length

$$L_\parallel\approx e^{\gamma\tilde{\xi}/k_BT}\sim|l_L-l_0|^{-1}\ , \tag{4.15}$$

which is the thermal analogue of (4.3).

C. Higher dimensions

The scaling arguments developed in the previous section are readily extended to higher dimensions. Consider first a directed polymer in d transverse dimensions confined between two parallel d-dimensional hyperplanes with average energies $-1/\alpha$ and $-1/\beta$. To treat the d-dimensional case, we only need to modify the fluctuation-induced energy gain in the kink energy estimate (4.2). Since the localized polymer is free to optimize its configuration parallel to the hyperplane, the energy fluctuations are reduced to $L_\parallel^\theta$, where $\theta=\theta_{d-1}\le\frac{1}{2}$ is the energy fluctuation exponent of a DPRM in $d-1$ transverse dimensions [5]. Repeating the arguments following Eq. (4.2), we find that the approach to the coexistence line is characterized by two diverging length scales

$$L_\parallel\sim|\alpha-\beta|^{-\nu_\parallel},L_\perp\sim|\alpha-\beta|^{-\nu_\perp}\ , \tag{4.16}$$

with the scaling exponents

$$\nu_\perp=\frac{\theta}{1-\theta},\nu_\parallel=\frac{\nu_\perp}{\theta}\ . \tag{4.17}$$

Similarly the (negative) confinement energy at coexistence scales as

$$-\Delta e\sim L^{-1/\nu_\perp}\ . \tag{4.18}$$

The one-dimensional exponents are recovered by setting $\theta=\frac{1}{2}$. In $d=2$, the value $\theta=\theta_1=\frac{1}{3}$ is known to be exact [5,8], and results in $\nu_\perp=\frac{1}{2},\nu_\parallel=\frac{3}{2}$. We may also note that the behavior in the thermal case can be viewed as the limiting case $\theta=0$ (no energy fluctuations) of (4.17): Then $L_\perp$ diverges logarithmically, $L_\parallel\sim|\alpha-\beta|^{-1}$ and Δe becomes exponentially small in L.

To illustrate some alternative confinement geometries, we focus on the physically most relevant case of $d=2$ transverse dimensions. Consider, e.g., a polymer confined to a tube of radius L. If the tube wall is sufficiently attractive, the polymer can explore the whole surface of the tube without traversing its inside; the switching phenomenon observed in $d=1$ is absent. Consequently, the confinement energy is that of a polymer in $d=1$ with periodic boundary conditions, i.e., $\Delta e\sim 1/L$ with a positive coefficient. On the other hand, if the wall of the tube is repulsive, the general result $\Delta e\sim L^{-\tau}$ is expected to apply, with $\tau=2(1-\zeta)/\zeta\approx 1.23$ [5,21] in $d=2$ (cf. Sec. III B). The same scaling holds for a polymer confined between two infinite repulsive planes.

We summarize these findings within the context of two-dimensional moving interfaces governed by the Kardar-Parisi-Zhang equation (2.19) [24]. Consider first an interface of lateral extension $L_x=L_y=L$. If the growth rate at the boundary is enhanced, the finite size correction to the overall growth velocity is positive and scales as $L^{1.23}$, as in the case of periodic boundary conditions [21]. If the growth rate is reduced at the boundaries the correction scales instead as L^{-1}. Finally, if $L_x\ll L_y$ and the growth rate at the long sides is reduced, the correction becomes negative and scales as $L_x^{-1/\nu_\perp}=L_x^{-2}$.

V. CONCLUSIONS AND OUTLOOK

Let us then recapitulate the main achievements of this work. Building upon the exact solution of the lattice gas problem due to Derrida, Domany, and co-workers [13–15], we have provided a detailed description of the unbinding of the (1+1)-dimensional DPRM from an attractive wall. The predictions obtained previously by the replica method [1,17] were confirmed, and additional features such as the appearance of a diverging correlation length on the *unbound* side of the transition, and the exact scaling form for the confinement energies, were found.

Guided by the occurrence of shock fluctuations in the lattice-gas model, we were further led to discover a novel type of critical phenomenon associated with the coexistence of two energetically degenerate bound phases. These *coexistence fluctuations* are unique to the confined geometry considered in this paper, and they are driven by the quenched disorder near the localizing boundaries. Compared to the effect of thermal fluctuations in the

same situation, the boundary disorder dramatically enhances the rate at which the directed polymer switches between the two bound phases: Rather than being exponentially small in the wall separation, it decays as an inverse power of L. We expect effects of this kind to be important for the behavior of flux line arrays in type II superconductors subject to both point disorder and extended defects [6]. Indeed, the hopping of vortices between defects of comparable energy is known to play a central role for the transport properties of these materials [34].

While our scaling picture for the coexistence fluctuations was easily extended to higher dimensions (Sec. IV C), we have little to say about the properties of the unbinding transition, such as the value of the unbinding exponent ψ, in transverse dimensionalities $d>1$. Nevertheless, some insight can be gained from reexamining the steps that lead to the exact result $\psi=2$ in $d=1$. In fact, this result is already inherent in the thermodynamics of the transition, discussed in Sec. III A, when combined with some simple scaling considerations. It is clear that the confinement of the polymer to the lateral length scale ξ in the bound phase incurs an excess energy per unit length of order $\xi^{-\tau}$, which has to be compensated by the attractive wall potential. If $\xi\sim|\alpha_c-\alpha|^{-\psi}$ when $\alpha\to\alpha_c$, it follows that the singular part of the energy vanishes as $|\alpha_c-\alpha|^{\psi\tau}$. Thus the quadratic behavior of the (macroscopic) ground state energy per unit length, together with the confinement energy exponent $\tau=1$, implies that $\psi=2/\tau=2$. In general $\tau=2(1-\zeta)/\zeta$, and hence the assumption that $\psi\tau=2$ implies the necklace model prediction [27]

$$\psi=\frac{\zeta}{1-\zeta}\ . \tag{5.1}$$

How general is the quadratic singularity of the ground state energy at the unbinding transition? It is instructive to recast this question in the language of interfaces evolving according to the KPZ equation (2.19). Specifically, consider a d-dimensional interface in a semi-infinite geometry which experiences a reduced growth rate [24] along the $(d-1)$-dimensional boundary. The unbinding transition corresponds to a transition from a ("bound") phase where the retardation at the boundary is sufficient to macroscopically tilt the interface, to a phase where the interface is oriented horizontally; the ground state energy singularity translates into the singularity of the growth rate (Sec. II). As a consequence of the Galilean invariance of the KPZ equation [4,9], the change in growth rate due to an imposed (small) tilt is always *quadratic* in the tilt, a statement that holds for arbitrary d. To be able to conclude that $\psi\tau=2$ in general, we would further have to argue that the interface tilt in the bound phase varies linearly with the (bare) boundary growth rate $\alpha_c-\alpha$. This is quite obviously the case in $d=1$, and can be most easily verified in the lattice gas representation, where it implies that the boundary parameters α and β directly control the boundary densities [12]. However, this simple scenario may well be due to the fluctuation-dissipation theorem (FDT) for the one-dimensional KPZ equation [5,7,9], which ensures short-range spatial correlations of the interface gradient (equivalently the lattice gas density). It is conceivable that the absence of an FDT in higher dimensions leads to a nontrival dependence of the interface tilt on the boundary potential and, therefore, to a value of the unbinding exponent that differs from (5.1). We hope to clarify this point in the near future.

ACKNOWLEDGMENTS

J.K. wishes to thank Gunter Schütz for a useful conversation, and for making available his unpublished work.

APPENDIX

In this appendix we derive expressions for the ground state energy per unit length e_0, which can be used to extract the leading-order finite-size corrections in the three different phases and on the phase boundaries.

From the mapping discussed in Sec. II we have

$$e_0(L)=-\tfrac{1}{2}J_{L-1}^{-1}\ , \tag{A1}$$

where [Eq. (57) of Ref. [14]]

$$J_N^{-1}=\frac{\langle W|C^N|V\rangle}{\langle W|C^{N-1}|V\rangle} \tag{A2}$$

is the inverse of the stationary lattice-gas current in a system of N sites.

To compute the matrix elements in (A2), we follow the discussion in Appendix B of Ref. [14]. There, an expression for $\langle W|C^N|V\rangle$ [Eq. (B10) of Ref. [14], hereafter referred to as Eq. (DEHP:B10); other equations in this reference will be cited in a similar way] was given explicitly only for $a\equiv\alpha^{-1}-1<1$ and $b\equiv\beta^{-1}-1<1$. For other values of a and b, one has to perform proper analytic continuations of (DEHP:B6) and (DEHP:B8). The first one is simple: writing $z=e^{i\theta}$, the integral in (DEHP:B6) is transformed to an integral over the unit circle on the complex z plane. The integrand has three poles, two simple poles at $z=b$ and $1/b$, and a third pole at the origin. It is easy to show that, in order for the integral to be equal to b^{k-1} in general, the integration contour S should enclose $z=0$ and b but not $1/b$. For z away from the unit circle, the proper extension of (DEHP:B3) is to replace $\sin k\theta$ with $(z^k-z^{-k})/(2i)$. In this form, the sum (DEHP:B8) converges to

$$L_a(z)=\frac{1}{2i}\left[\frac{1}{z^{-1}-a}-\frac{1}{z-a}\right]\ , \tag{A3}$$

provided $a<\min\{|z|,|z|^{-1}\}$. Thus, the contour S should enclose also $z=a$ but not $z=1/a$. Summarizing, we have

$$\langle W|C^N|V\rangle=\frac{\alpha+\beta-1}{\alpha\beta}\oint_S dz f_N(z)\ , \tag{A4}$$

where

$$f_N(z)=-\frac{1}{4\pi i}\frac{z(z-z^{-1})^2(2+z+z^{-1})^N}{ab(z-a)(z-a^{-1})(z-b)(z-b^{-1})}\ . \tag{A5}$$

The integration contour S encloses $z=0$ and two of the simple poles of f_N at $z=a$ and b, but not the ones at $z=a^{-1}$ and b^{-1}.

To evaluate (A4) in the limit of large N, we rewrite the integral as

$$\langle W|C^N|V\rangle=\frac{\alpha+\beta-1}{\alpha\beta}[I_1(N)+I_2(N)+I_3(N)]\ , \tag{A6}$$

where

$$I_1(N)=\int_{-\pi}^{\pi}\frac{d\theta}{\pi}\frac{\sin^2\theta[2(1+\cos\theta)]^N}{(1-2a\cos\theta+a^2)(1-2b\cos\theta+b^2)}\ ; \tag{A7}$$

$$I_2(N)=\begin{cases}0\ , & \text{if } a\le 1(\alpha\ge\frac{1}{2})\ ,\\ \oint_{S_1}dz\,f_N(z)-\oint_{S_2}dz\,f_N(z), & \text{otherwise;}\end{cases} \tag{A8}$$

$$I_3(N)=\begin{cases}0, & \text{if } b\le 1(\beta\ge\frac{1}{2})\ ,\\ \oint_{S_3}dz\,f_N(z)-\oint_{S_4}dz\,f_N(z), & \text{otherwise.}\end{cases} \tag{A9}$$

Here S_1, S_2, S_3, and S_4 are closed contours, each enclosing only a single pole at $z=a$, a^{-1}, b, and b^{-1}, respectively. Using the residue theorem, the integrals in (A8) and (A9) can be easily evaluated. The results are given by, for $\alpha\neq\beta,1-\beta$,

$$I_2(N)=\frac{(1-2\alpha)\alpha^2\beta^2}{(\beta-\alpha)(\alpha+\beta-1)}[\alpha(1-\alpha)]^{-N-1},\quad(\alpha<\tfrac{1}{2}), \tag{A10}$$

$$I_3(N)=\frac{(1-2\beta)\alpha^2\beta^2}{(\alpha-\beta)(\alpha+\beta-1)}[\beta(1-\beta)]^{-N-1},\quad(\beta<\tfrac{1}{2}). \tag{A11}$$

Consider now Eq. (A7). For $N\gg1$, the integrand is peaked at $\theta=0$, with a width of order $N^{-1/2}$ and exponential tails at $|\theta|>N^{-1/2}$. Expanding $\sin\theta$ and $\cos\theta$ around $\theta=0$ and keeping only terms up to second order in suitable form, we obtain

$$I_1(N)\simeq\int_{-\infty}^{\infty}\frac{d\theta}{\pi}\frac{\theta^2 4^N\exp(-\frac{1}{4}N\theta^2)}{[(1-a)^2+a\theta^2][(1-b)^2+b\theta^2]}\ . \tag{A12}$$

The correction to (A12) is by a factor N^{-1} smaller. Setting

$$u^2=\frac{N(1-a)^2}{4a}=\frac{N(1-2\alpha)^2}{4\alpha(1-\alpha)} \tag{A13}$$

and

$$v^2=\frac{N(1-b)^2}{4b}=\frac{N(1-2\beta)^2}{4\beta(1-\beta)}\ , \tag{A14}$$

Eq. (A12) can be rewritten as

$$I_1(N)\simeq\frac{2\alpha^2\beta^2}{(\alpha-\beta)(\alpha+\beta-1)}N^{-1/2}4^N[F(u)-F(v)]\ , \tag{A15}$$

where

$$F(x)=x^2\int_{-\infty}^{\infty}\frac{dy}{\pi}\frac{1}{x^2+y^2}\exp(-y^2)\ . \tag{A16}$$

The integral on the right-hand side of (A16) can be expressed in terms of the error function by making the substitution

$$\frac{1}{x^2+y^2}=\int_0^{\infty}ds\,\exp[-s(x^2+y^2)]\ . \tag{A17}$$

Carrying out the integration over y and some elementary manipulations we obtain

$$F(x)=|x|\exp(x^2)[1-\mathrm{erf}(|x|)]\ , \tag{A18}$$

where

$$\mathrm{erf}(x)=\frac{2}{\sqrt{\pi}}\int_0^x dy\,\exp(-y^2)\ . \tag{A19}$$

The limiting behaviors of $F(x)$ are given by

$$F(x)=\begin{cases}|x|+O(x^2), & x\to0\ ; \qquad (A20)\\ \frac{1}{\sqrt{\pi}}[1-\frac{1}{2}x^{-2}+O(x^{-4})], & x\to\infty\ . \qquad (A21)\end{cases}$$

[1] G. Forgacs, R. Lipowsky, and Th. M. Nieuwenhuizen, in *Phase Transitions and Critical Phenomena,* edited by C. Domb and J. L. Lebowitz (Academic, London, 1991), Vol. 14, p. 135.

[2] L.-H. Tang and I. F. Lyuksyutov, Phys. Rev. Lett. **71**, 2745 (1993); L. Balents and M. Kardar, Europhys. Lett. **23**, 503 (1993); and unpublished.

[3] M. Kardar and Y. C. Zhang, Phys. Rev. Lett. **58**, 2087 (1987).

[4] D. S. Fisher and D. A. Huse, Phys. Rev. B **43**, 10728 (1991).

[5] For a review see J. Krug and H. Spohn, in *Solids Far From Equilibrium,* edited by C. Godrèche (Cambridge University Press, Cambridge, England, 1991), p. 479.

[6] T. Hwa, D. R. Nelson, and V. M. Vinokur, Phys. Rev. B **48**, 1167 (1993); I. Arsenin, T. Halpin-Healy, and J. Krug, Phys. Rev. E **49**, 3561 (1994).

[7] D. A. Huse, C. L. Henley, and D. S. Fisher, Phys. Rev. Lett. **54**, 2924 (1985).

[8] M. Kardar, G. Parisi, and Y. C. Zhang, Phys. Rev. Lett. **56**, 889 (1986).

[9] E. Medina, T. Hwa, M. Kardar, and Y. C. Zhang, Phys. Rev. A **39**, 3053 (1989).

[10] H. Kesten, *Lecture Notes in Mathematics* (Springer, Berlin, 1986), Vol. 1180.

[11] L.-H. Tang, J. Kertész, and D. E. Wolf, J. Phys. A **24**,

L1193 (1991).
[12] J. Krug, Phys. Rev. Lett. **67**, 1882 (1991).
[13] B. Derrida, E. Domany, and D. Mukamel, J. Stat. Phys. **69**, 667 (1992).
[14] B. Derrida, M. R. Evans, V. Hakim, and V. Pasquier, J. Phys. A **26**, 1493 (1993).
[15] G. Schütz and E. Domany, J. Stat. Phys. **72**, 277 (1993).
[16] Our approach is complementary to the work of M. Henkel and G. Schütz, Physica A **206**, 187 (1994), who map the nonequilibrium lattice gas onto an equilibrium vertex model *without* disorder.
[17] M. Kardar, Phys. Rev. Lett. **55**, 2235 (1985); Nucl. Phys. B **290**, 582 (1987).
[18] J. Wuttke and R. Lipowsky, Phys. Rev. B **44**, 13 042 (1991).
[19] M. Zapotocky and T. Halpin-Healy, Phys. Rev. Lett. **67**, 3463 (1991).
[20] V. Privman and N. M. Svrakić, Phys. Rev. B **37**, 3713 (1988); see also P. J. Upton, *ibid.* **44**, 10 335 (1991).
[21] J. Krug and P. Meakin, J. Phys. A **23**, L987 (1990).
[22] D. A. Huse and C. L. Henley, Phys. Rev. Lett. **54**, 2708 (1985).
[23] P. Meakin, P. Ramanlal, L. M. Sander, and R. C. Ball, Phys. Rev. A **34**, 5091 (1986); M. Plischke, Z. Rácz, and D. Liu, Phys. Rev. B **35**, 3485 (1987).
[24] For interface growth the sign of the nonlinearity in (2.19) can be either positive or negative [5,11,21,25,28]. If it is positive the roles of attractive and repulsive boundary potentials are reversed [31].
[25] L.-H. Tang, B. M. Forrest, and D. E. Wolf, Phys. Rev. A **45**, 7162 (1992).
[26] H. van Beijeren, R. Kutner, and H. Spohn, Phys. Rev. Lett. **54**, 2026 (1985).
[27] R. Lipowsky and M. E. Fisher, Phys. Rev. Lett. **56**, 472 (1986); Phys. Rev. B **36**, 2126 (1987).
[28] J. Krug, P. Meakin, and T. Halpin-Healy, Phys. Rev. A **45**, 638 (1992).
[29] The result $c = \frac{3}{2}$ in the unbound phase was conjectured in Ref. [21].
[30] J. Krug, in *Spontaneous Formation of Space-Time Structures and Criticality*, edited by T. Riste and D. Sherrington (Kluwer, Amsterdam, 1991), p. 37.
[31] D. E. Wolf and L. H. Tang, Phys. Rev. Lett. **65**, 1591 (1990).
[32] B. Derrida, S. A. Janowsky, J. L. Lebowitz, and E. R. Speer, Europhys. Lett. **22**, 651 (1993).
[33] G. Schütz, Phys. Rev. E **47**, 4265 (1993).
[34] D. R. Nelson and V. M. Vinokur, Phys. Rev. B **48**, 13 060 (1993).

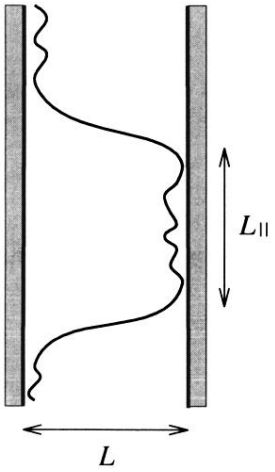

FIG. 5. Sketch of a kink excitation of a polymer bound at the (slightly more attractive) left wall.